Mon. Not. R. Astron. Soc. **359,** 615–623 (2005) doi:10.1111/j.1365-2966.2005.08925.x

On the origin of the radial mass density profile of the Galactic halo globular cluster system

Geneviève Parmentier★† and Eva K. Grebel

Astronomical Institute, University of Basel, 7 Venusstrasse, CH-4102 Binningen, Switzerland

Accepted 2005 February 14. Received 2005 January 19; in original form 2004 September 22

ABSTRACT

We investigate what may be the origin of the presently observed spatial distribution of the mass of the Galactic Old Halo globular cluster system. We propose its radial mass density profile to be a relic of the distribution of the cold baryonic material in the protogalaxy. Assuming that this one arises from the profile of the whole protogalaxy minus the contribution of the dark matter (and a small contribution of the hot gas by which the protoglobular clouds were bound), we show that the mass distributions around the Galactic centre of this cold gas and of the Old Halo agree satisfactorily. In order to demonstrate our hypothesis even more conclusively, we simulate the evolution with time, up to an age of 15 Gyr, of a putative globular cluster system whose initial mass distribution in the Galactic halo follows the profile of the cold protogalactic gas. We show that beyond a galactocentric distance of order 2–3 kpc, the initial shape of such a mass density profile is preserved despite the complete destruction of some globular clusters and the partial evaporation of some others. This result is almost independent of the choice of the initial mass function for the globular clusters, which is still ill determined. The shape of these evolved cluster system mass density profiles also agrees with the presently observed profile of the Old Halo globular cluster system, thus strengthening our hypothesis. Our result might suggest that the flattening shown by the Old Halo mass density profile at short distances from the Galactic centre is, at least partly, of primordial origin.

Key words: Galaxy: formation – globular clusters: general – Galaxy: halo.

1 INTRODUCTION

Globular clusters (GCs) are thought to be the oldest bound stellar systems in our Galaxy. Their study therefore provides valuable information about the early Galactic evolution. In this respect, a major problem is that we do not know whether what we presently observe is still representative of the initial conditions and, thus, a fossil imprint of the formation process, or whether the initial conditions have been wiped out by a 15-Gyr long evolution within the tidal fields of the Milky Way. Modelling the dynamical evolution of the Galactic globular cluster system (GCS) is thus of great interest as it helps us to go back in time to the earliest stages of the cluster system and to disentangle the formation and evolutionary fingerprints (see, e.g. Gnedin & Ostriker 1997; Baumgardt 1998; Vesperini 1998; Fall & Zhang 2001). The GCs most vulnerable to evaporation and disruption are the low-mass clusters located at small galactocentric distance. As a result, the evolution with time of a GCS is markedly determined by the initial distribution of the GCs in space around the Galactic centre as well as by their initial mass spectrum.

As for the presently observed spatial distribution of the Galactic halo GCs, it is centrally concentrated with the density varying as $D^{-3.5}$ (D is the Galactocentric distance) over most of the halo (Zinn 1985). In the inner 3–4 kpc, the distribution flattens to something closer to an D^{-2} dependence. As a result, the overall distribution is conveniently described by a power law with a core (see Section 2). The observed central flattening probably arises from a combination of several effects: our failure to discover some GCs in the heavily absorbed central regions of the Galaxy, distance errors and the real flattening of the distribution. It is still unclear whether such a flattening is of primordial origin and reflects the initial spatial distribution of the system, or whether it has been completely determined by evolutionary processes. The latter are especially effective at small galactocentric distances where the GC relaxation time is short, causing the disruption of some GCs and the partial evaporation of some others. More generally, as far as we are aware of, the shape of the whole spatial distribution of the halo GCS has received no explanation.

The aim of this paper is to present a possible model accounting for the distribution around the Galactic centre of the mass content of the halo GCS, that is, the variation with galactocentric distance

★E-mail: gparm@ast.cam.ac.uk

†Present address: Institute of Astronomy, University of Cambridge, Madingley Road, Cambridge CB3 0HA.

of the mass density of the halo GCS. We will consider solely the Old Halo (OH) GCs, excluding from our analysis the Younger Halo (YH) subsystem. This one is made of GCs suspected of having been accreted and is thus of limited relevance to the earliest stages of the main body of our Galaxy (see, e.g. Zinn 1993; van den Bergh 1993). A common trend of different scenarios for the formation of GCs is to assume that their gaseous progenitor clouds, whatever their size ($\sim 10^6\,M_\odot$, e.g. Fall & Rees 1985; $\sim 10^9\,M_\odot$, e.g. Harris & Pudritz 1994), are embedded in a hot and tenuous background at the virial temperature. We build on this picture, splitting the protogalaxy in a set of three components: a gaseous medium consisting of hot and cold phases (in the form of a collection of cold and dense clouds, the gaseous precursors of the halo GCs, pressure bound by a hot medium), and a dark matter corona. We investigate whether the mass density profile of the halo GCS may trace the profile of the cold phase, that is, of the cold baryonic matter which was available to star formation some 15-Gyr ago.

The outline of the paper is as follows. In Section 2, we build the radial mass density profile of the OH and obtain new fits of a power law with a core, with parameter values appropriate to this subsystem of GCs only. We also summarize the evidence from the literature following which mass-related quantities may be better probes to the initial conditions than number related quantities. In Section 3, we present our hypothesis regarding the shape of the initial mass density profile of the OH GCS and we compare the OH profile obtained in Section 2 with our suggested model, that is, with the radial density profile of the cold protogalactic material. In Section 4, we simulate the evolution with time of a GCS whose initial mass density profile mirrors that of the cold protogalactic gas, and this for various initial GC mass spectra. We compare the spatial mass distributions of these evolved systems with the presently observed spatial mass distribution of the OH. Finally, our conclusions are presented in Section 5.

2 RADIAL DISTRIBUTION OF THE HALO GLOBULAR CLUSTER SYSTEM MASS

The observed radial distribution of the Galactic GCS (i.e. the number of GCs per unit volume in space as a function of Galactocentric distance D) is often parametrized by a simple power law with a core

$$\rho(D) = \rho_0 \left(1 + \frac{D}{D_\mathrm{c}}\right)^{-\gamma}. \quad (1)$$

Realizing a 'chi-by-eye' fitting of this type of curve on the observed spatial distribution of the GCS, Djorgovski & Meylan (1994) found good matches for $\gamma \sim 3.5$–4.0 and $D_\mathrm{c} \sim 0.5$–2 kpc, the steepest slope being associated with the largest core. This approach is purely empirical, however, and is not meant to imply any physical meaning of the distribution given by equation (1).

Both the number and the mass density profiles of the halo ([Fe/H] < -0.8) GCS can be described by equation (1), as both profiles are indistinguishable in shape. However, as argued by McLaughlin (1999), the spatial distribution of the mass is likely to be a better estimate of the initial conditions than its number counterpart. Dynamical evolution targetting mostly low-mass clusters and those accounting for a limited fraction of the GCS mass (see below and Section 4), the decrease with time of the total GCS mass is much slower than the decrease of the total number of GCs.

This interesting property comes from how the shape of the initial mass spectrum of the halo GCs may have looked like. In our Galaxy, the luminosity function of the halo GCs [1] (the number of GCs per unit absolute magnitude, which is proportional to the number of objects per logarithmic mass interval) is bell shaped and usually fitted with a Gaussian. However, the underlying mass spectrum (i.e. the number of objects per linear mass interval) is well fitted by a two-index power law, with exponents ~ -2 and ~ -0.2 above and below $\sim 1.5 \times 10^5\,M_\odot$, respectively (McLaughlin 1994). The peak of the Gaussian magnitude function in fact coincides with the cluster mass at which the slope of the mass spectrum changes. The slope of the high-mass regime is reminiscent of what is observed in interacting and merging galaxies (see, e.g. Whitmore & Schweizer 1995; Whitmore et al. 2002) where systems of young GCs show a well-defined power law with slopes ranging between -1.8 and -2 for their luminosity spectrum (but see the discussion in Section 4). This thus suggests that the initial mass spectrum of the halo GCS may have been itself a single power law. Numerous studies of GCS dynamical evolution modelling have shown that a Hubble time long evolution turns such an initial spectrum into the presently observed one (e.g. Baumgardt 1998; Vesperini 1998; Fall & Zhang 2001). In fact, with low-mass clusters being the most vulnerable to evaporation and disruption, the GC mass spectrum gets severely depleted below a turnover of $\sim 1.5 \times 10^5\,M_\odot$, leading to a much shallower mass spectrum (i.e. slope $\simeq -0.2$) in the low-mass regime. Pal 5 constitutes a striking example of a low-mass GC currently dissolved by Galactic tidal fields (Odenkirchen et al. 2001; Dehnen et al. 2004).

Assuming that most of the GCs more massive than the turnover are spared by the dynamical evolution, McLaughlin (1999) compares the GCS initial and final mass spectra (i.e. the single power law with the two-index power law) and derives useful formulae to estimate the fraction of surviving clusters, both in terms of mass and numbers (his equations 4–7). His results show that mass-related quantities are reasonably preserved by a Hubble time long evolution, even though low-mass GCs are disrupted in large numbers. Considering the specific case of the Milky Way (power-law slopes of -0.2 and of around -1.8 to -2.0 for the low- and high-mass regimes, respectively, a turn-off mass of $1.5 \times 10^5\,M_\odot$, and lower and upper mass limits of $10^4\,M_\odot$ and $10^6\,M_\odot$, respectively), the application of his formulae shows that the initial mass of the GCS is decreased by 40 per cent, while the fraction of surviving clusters is 16 per cent. In the case of a lower limit for the cluster initial mass range, say $10^3\,M_\odot$, the contrast between the decreases in mass and number is even more striking, i.e. the survivors still represent 44 per cent of the initial total mass but 2 per cent of the initial number only. The formulae of McLaughlin (1999) thus illustrate that, compared to number related quantities, mass-related quantities are less markedly affected by a 15-Gyr long evolution. As a result, the radial mass density profile of the halo GCS may be considered as a reasonably reliable estimator of their initial distribution around the Galactic centre. We will make this point more quantitative in Section 4 and show that such an hypothesis is indeed robust.

In this paper, we are interested in understanding the origin of the initial spatial distribution of the halo GCS mass within the Milky Way, which we approximate by the presently observed mass density profile at this stage of the discussion. We do not consider the

[1] In what follows, we adopt the nomenclature of McLaughlin & Pudritz (1996). We call the mass/luminosity *spectrum* the number of objects per *linear* luminosity/mass interval, dN/dm or dN/dL, while we refer to the mass/luminosity *function* to describe the number of objects per *logarithmic* luminosity/mass interval, dN/d log m or dN/d log L.

Table 1. OH sample.

NGC 288	NGC 5286	NGC 5986	NGC 6218	NGC 6293	HP1	NGC 6522	NGC 6638	NGC 6752
Pal2	NGC 5466	NGC 6093	NGC 6235	NGC 6341	NGC 6362	NGC 6535	NGC 6652	NGC 6779
NGC 1904	NGC 5634	NGC 6121	NGC 6254	NGC 6325	NGC 6402	NGC 6540	NGC 6656	NGC 6809
NGC 2298	NGC 5694	NGC 6101	Pal15	NGC 6333	NGC 6401	NGC 6544	NGC 6681	NGC 6864
NGC 4372	NGC 5824	NGC 6144	NGC 6266	NGC 6355	NGC 6397	NGC 6541	NGC 6712	NGC 7078
NGC 4833	NGC 5897	NGC 6139	NGC 6273	IC1257	NGC 6426	NGC 6558	NGC 6717	NGC 7089
NGC 5024	NGC 5904	NGC 6171	NGC 6284	NGC 6366	NGC 6453	NGC 6569	NGC 6723	NGC 7099
NGC 5053	NGC 5946	NGC 6205	NGC 6287	Ter4	NGC 6517	NGC 6626	NGC 6749	NGC 7492

more metal-rich, presumably second generation, bulge/disc GCs ([Fe/H] $\geqslant -0.8$). In addition, the halo ([Fe/H] < -0.8) subsystem itself could be divided into two groups, traditionally referred to as the OH and the YH (see, e.g. Zinn 1993; van den Bergh 1993; Mackey & Gilmore 2004). Evidence supporting the existence of such two distinct halo subsystems have been accumulating over the past years. OH and YH GCs show differences in horizontal branch morphology, age, kinematics, spatial distribution (see Parmentier et al. 2000, their Section 2, for a review), as well as differences in the distribution of their core radius (Mackey & Gilmore 2004). The properties of the OH group are consistent with the majority of its members having been formed in situ during the large-scale collapse of the protogalactic cloud, as envisioned by Eggen, Lynden-Bell & Sandage (1962). On the other hand, the YH GCs are not native to the Galaxy, probably having been formed in external dwarf galaxies and afterwards accreted into the outer halo while their host galaxies were being swallowed by the Milky Way, as suggested by Searle & Zinn (1978). The current accretion of the Sagittarius dwarf galaxy and of its small GCS is the smoking gun of this process. As we are interested in the mass density profile of the GCS which formed within the original potential well of the Galaxy, we restrict our attention to the OH GCs. This OH/YH division has already been proven most fruitful as the OH GCS shows a metallicity gradient and obeys a mass–metallicity relation, features predicted by simple self-enrichment models (Parmentier et al. 2000 and Parmentier & Gilmore 2001, respectively), while the whole halo GCS (OH+YH) does not.

Lists of OH and YH GCs are provided in Lee, Demarque & Zinn (1994) and Da Costa & Armandroff (1995). With respect to these, we have made two slight changes, however. In our present OH sample, we ignore NGC 2419. Although coeval with the inner halo (Harris et al. 1997; Salaris & Weiss 2002), this GC is located at a galactocentric distance of order 90 kpc and is thus unlikely to belong to the main body of the Galaxy. Moreover, van den Bergh & Mackey (2004) show that NGC 2419 and ω Cen on the one hand, and the other halo GCs on the other hand, are at different locii in a half-light radius versus an absolute visual magnitude diagram. They thus suggest that, as ω Cen (which we also exclude from our sample), NGC 2419 might be the tidally stripped core of a former dwarf spheroidal galaxy. An efficient tidal stripping would, however, require NGC 2419 to cross the inner Galactic regions. Unfortunately, its orbit is still ill determined. Also, unlike ω Cen, there is no evidence for a metallicity spread among the cluster giants. If NGC 2419 is actually the remnant of a former dwarf galaxy, the parent galaxy might, like the Ursa Minor dwarf galaxy (van den Bergh 2000), have produced a single generation of metal-poor stars. Bearing these caveats in mind, we thus note that the main peculiarity of NGC 2419 with respect to the bulk of the OH is its large galactocentric distance. Neglecting NGC 2419, the OH is thoroughly contained within $D \leqslant 40$ kpc. Additionally, we have moved the cluster NGC 6864 from the YH group to the OH group. According to the former (1999) edition of the GC McMaster Catalog (Harris 1996), the metallicity and the horizontal branch ratio (HBR) of NGC 6864 are 1.32 and 0.42, respectively. The updated (2003) values being [Fe/H] = 1.16 and HBR = 0.07, the location of this cluster in the [Fe/H] versus HBR diagram shows that it is more likely to be a member of the OH group rather than a YH GC. Finally, about 25 halo GCs of the Harris Catalogue still miss HB index measurements. Using recently published colour–magnitude diagrams, (e.g. Piotto et al. 2002), Mackey & Gilmore (2004) have sorted most of these yet undefined GCs. All the GCs to which Mackey & Gilmore (2004) have assigned an OH membership have been added to our OH sample. This one is presented in Table 1.

Before proceeding any further, we derive estimates for the parameters γ and D_c appropriate for the sole OH, as previous fits refer to either the whole Galactic GCS or the whole halo system, thus ignoring their heterogeneity. We fit

$$\log_{10}\rho(D) = \log_{10}\rho_0 - \gamma \log_{10}\left(1 + \frac{D}{D_c}\right) \quad (2)$$

to the observed OH mass density distribution through a Levenberg–Marquardt algorithm (Press et al. 1992). Our source for the galactocentric distances D and the absolute visual magnitudes M_v is the McMaster database compiled and maintained by Harris (1996, updated February 2003). Cluster absolute visual magnitudes have been turned into luminous mass estimates by assuming a constant mass-to-light ratio $m/L_v = 2.35$. This value corresponds to the average of the mass-to-light ratios of the halo GCs for which Pryor & Meylan (1993) derived dynamical mass estimates. The mean m/L_v is almost independent of the halo group considered, that is, OH or OH+YH.

The OH mass profile is derived by binning the data with two different bin sizes: $\Delta\log D = 0.1$ and 0.2 (D is in kpc), corresponding to 16 and 8 points, respectively. As for the size of the error bars, a Poissonian error on the number of GCs in each bin is combined with a fixed error on the mass-to-light ratio. In fact, not all GCs show the same mass-to-light ratios, the standard deviation in the Pryor & Meylan (1993) compilation being of order $\sigma_{\log(M/L_v)} = 0.17$.

The results of the fitting procedure are presented in Table 2 and superposed to the observed distribution in Fig. 1. For each fit, we also give the χ^2 and the incomplete gamma function $Q(\nu/2, \chi^2/2)$ (ν is the number of degrees of freedom) which provides a quantitative measure for the goodness-of-fit of the model[2] (Press et al. 1992). Keeping all three parameters free, we obtain a slope much steeper ($\gamma \simeq -5$) than suggested by previous works ($\gamma \simeq -3.5$ to -4.0; Zinn 1985; Djorgovski & Meylan 1994).

[2] We remind the reader that a Q value of 0.1 or larger indicates satisfactory agreement between the model and the data.

Table 2. Results of fitting a power law with a core on the observed mass density profile of the OH subsystem.

$\Delta\log D$	$\log_{10}(\rho_0)$	D_c	$-\gamma$	χ^2	Q
0.1	5.6 ± 0.3	3.7 ± 2.0	-5.1 ± 0.9	11.7	0.55
0.2	5.6 ± 0.4	3.5 ± 2.4	-4.9 ± 1.1	3.8	0.58
			γ imposed		
0.1	6.4 ± 0.4	0.9 ± 0.3	-3.5	17.7	0.22
0.2	6.3 ± 0.5	1.0 ± 0.4	-3.5	7.0	0.32
0.1	6.0 ± 0.3	1.7 ± 0.4	-4.0	13.9	0.46
0.2	5.9 ± 0.3	1.9 ± 0.5	-4.0	4.8	0.57

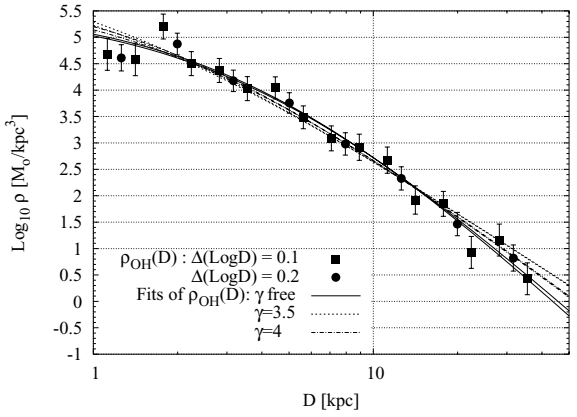

Figure 1. Fits of a power law with a core on the observed mass density profile of the OH subsystem. The different curves correspond to the values of the parameters as given in Table 2.

Our slope is coupled with a rather large core ($D_c \simeq 3.6$ kpc), however. In fact, functions like equation (1) or (2) show a core-slope degeneracy in the sense that two distinct fits can provide a satisfactory agreement with the data provided that a steeper slope is associated with a larger core. This is also reflected by the large error bars for D_c and γ. Therefore, when describing a density profile through equation (1) or (2), it is important to quote the slope as well as the core length. We have thus performed additional fits in which the value of the exponent is set to values previously quoted in the literature, i.e. 3.5 and 4. Such shallower slopes again provide satisfactory agreement with the data, as indicated in Table 2. With respect to Djorgovski & Meylan (1994), who fitted the whole Galactic GCS (i.e. disc plus halo), core sizes are not markedly different.

3 ORIGIN OF THE OH GLOBULAR CLUSTER SYSTEM MASS DENSITY PROFILE

As already mentioned, the description of the OH GCS by equations (1) or (2) is purely empirical and does not imply any physical meaning. As far as we are aware of, no explanation has been put forward to explain the shape of the radial mass density profile $\rho_{OH}(D)$. In this paper, we propose that $\rho_{OH}(D)$ is tracing the mass distribution of the gas which, some 15-Gyr ago, was available to the process of star formation.

In the dark matter potential well, the protogalactic gas probably settles into a two-phase medium consisting of (1) a hot and tenuous gas at the virial temperature, $T_{hot} = 1.7 \times 10^6$ K and (2) a collection of much colder self-gravitating clouds, pressure bound by the hot medium in which they are embedded. These cold and dense clouds are often considered as the formation sites of the halo stars and GCs. In fact, this description of the protogalaxy is encountered in widely different pictures for halo GC formation. For instance, in the frame of the Galaxy formation model relying on a monolithic collapse, Fall & Rees (1985) suggested that the development of such a two-phase medium is promoted by thermal instability. On the other hand, adopting the hierarchical picture of Galaxy formation as the framework of their model, Harris & Pudritz (1994) proposed that the formation of GCs took place in the densest parts of large protogalactic fragments, of mass 10^8–10^9 $M_\odot$ (i.e. their supergiant molecular clouds, SGMCs), these SGMCs being, as in the Fall & Rees (1985) model, embedded in a hot background at the virial temperature.

We thus assume that the protogalaxy includes three components: a dark matter corona and a set of star-forming clouds embedded in a hot and diffuse background, and we write

$$\rho_{Gal}(D) = \rho_{cold}(D) + \rho_{hot}(D) + \rho_{DM}(D). \quad (3)$$

In this equation, ρ_{Gal}, ρ_{cold}, ρ_{hot} and ρ_{DM} are the mass densities of the protogalaxy, the cold phase, the hot phase and the dark matter, respectively.

The density profile ρ_{Gal} of the protogalaxy is conveniently described as a singular isothermal sphere

$$\rho_{Gal} = \frac{V_c^2}{4\pi G}\,\frac{1}{D^2}\,, \quad (4)$$

where V_c is the circular velocity of the gas in the dark matter potential well of the Galaxy and G is the gravitational constant. As we are mainly interested in the proto-Milky Way, we adopt $V_c = 220\,\mathrm{km\,s^{-1}}$.

Although physically unmotivated, we adopt the usual description of the spatial distribution of the dark matter mass in the Galaxy, that is

$$\rho_{DM}(D) = \frac{\rho_{0DM}}{1 + (D/D_{DM})^2}\,. \quad (5)$$

As for the central density and the softening length, we adopt the values of the Caldwell & Ostriker (1981) model $\rho_{0DM} = 13.72 \times 10^6\,M_\odot\,\mathrm{kpc^{-3}}$ and $D_{DM} = 7.8151$ kpc.

Regarding the hot gas confining the protoglobular clouds, its pressure profile is expected to scale as D^{-2} (e.g. Murray & Lin 1992; Harris & Pudritz 1994)

$$P_{hot}(D) = \frac{1.25 \times 10^{-9}}{D_{kpc}^2}\,\mathrm{dyne\,cm^{-2}}\,, \quad (6)$$

where the coefficient comes from Murray & Lin (1992).

Combining equation (6) with the virial temperature T_{hot}, we obtain the mass density profile of the hot tenuous gas

$$\rho_{hot}(D) = \frac{\rho_{0hot}}{D^2} = \frac{78.38}{D_{kpc}^2} \times 10^6\,M_\odot\,\mathrm{kpc^{-3}}. \quad (7)$$

The combination of equations (3), (4), (5) and (7) provides us with an estimate of the radial mass density profile of the cold gas, that is, the gas out of which halo GCs presumably formed

$$\rho_{cold}(D) = \left[\frac{890.7}{D^2} - \frac{78.4}{D^2} - \frac{13.7}{1 + (D/7.8)^2}\right] \times 10^6\,M_\odot\,\mathrm{kpc^{-3}}. \quad (8)$$

Fig. 2 displays equation (8), as well as the observed mass density profile of the OH GCS. The best (in a least-squares sense) agreement with the observed profile is obtained when the density of the protogalactic cold gas is scaled downwards by a factor 2×10^{-4}. χ^2 and Q values for the two bin sizes are provided in Table 3 (case a).

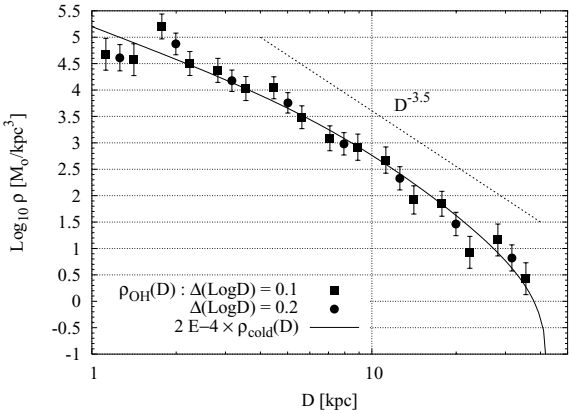

Figure 2. Fit of the model $\rho_{\rm cold}(D)$ (equation 8) to the presently observed mass density profile of the OH subsystem. The best (in the χ^2 sense) fit is obtained when a downwards scaling of 2×10^{-4} is applied to $\rho_{\rm cold}(D)$.

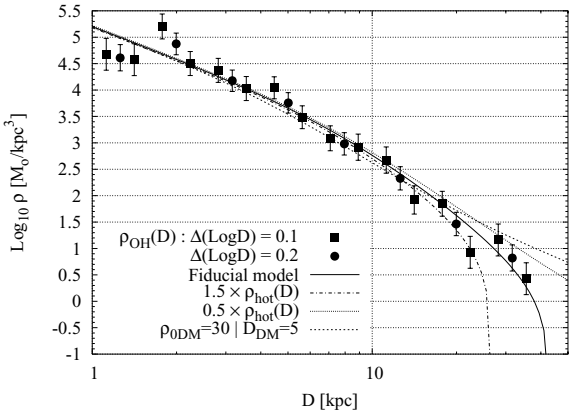

Figure 3. Comparison between the radial mass density profile of the OH subsystem and the model mass density $\rho_{\rm cold}(D)$, considering different values for the coefficients in equation (8).

Table 3. Results of fitting the spatial distribution of the baryonic cold matter (equation 8) on the observed mass density profile of the OH subsystem: (a) all the GCs defined as OH objects on the basis of their location in a [Fe/H] versus HBR diagram (Table 1 and Figs 1–3); (b) same as (a) but excluding five GCs with extended structures (filled symbols in Fig. 4); (c) same as (a) but excluding objects with extended structure or extreme kinematics (open symbols in Fig. 4) (see text for details).

	$\Delta\log_{10} D$	$\Delta\log_{10}\rho$	χ^2	Q
(a)	0.1	-3.69 ± 0.06	15.0	0.45
	0.2	-3.70 ± 0.08	6.3	0.51
(b)	0.1	-3.70 ± 0.06	14.5	0.49
	0.2	-3.71 ± 0.08	6.3	0.50
(c)	0.1	-3.78 ± 0.07	20.6	0.11
	0.2	-3.81 ± 0.08	11.1	0.14

Obviously, the shape of $\rho_{\rm cold}(D)$ provides a good fit to the observed distribution of the OH mass in our Galaxy. The factor 2×10^{-4} thus represents the formation efficiency of the halo bound stellar clusters which have managed to survive a Hubble time in the tidal fields of the Milky Way. This factor of course represents a lower bound to the GC primordial formation efficiency. As already highlighted by McLaughlin (1999), the next Section confirms that this one is unlikely to have been exceedingly larger.

Additionally, we note that the model, as described by equation (8), fits nicely the extent of the OH, as the cold gas density drops sharply at $D \simeq 40$ kpc. The outer limit of the OH would thus arise from the depletion of cold gas at this galactocentric distance. However, we note that this agreement may be a mere coincidence only as it heavily depends on the choice of the parameters $\rho_{0\rm hot}$, $\rho_{0\rm DM}$ and $D_{\rm DM}$ in equation (8). Fig. 3 illustrates how variations in the adopted values of the parameters affect the shape of the cold gas profile. The dashed-dotted and dotted curves represent equation (8) with the hot gas coefficient $\rho_{0\rm hot}$ increased and reduced by 50 per cent, respectively, while the dashed curve shows $\rho_{\rm cold}(D)$ if the dark matter coefficients of Caldwell & Ostriker (1981) are replaced by $\rho_{0\rm DM} = 30 \times 10^6\,{\rm M}_\odot\,{\rm kpc}^{-3}$ and $D_{\rm DM} = 5$ kpc (e.g. Baumgardt 1998). In the last two cases, the gas density decreases smoothly with galactocentric distance, without any sharp drop in the gas density. In that case, the outer limit of the OH might characterize a gas density threshold below which the formation of bound clusters is either inhibited or delayed. In the first case, the gas density drops sharply at closer galactocentric distance (i.e. $D \simeq 25$ kpc). Nevertheless, we emphasize that all four curves fit well the observed OH profile in the range 1–20 kpc, thus accounting for the vast majority of the OH GCs (less than 10 per cent of the OH GCs are located beyond $D \simeq 20$ kpc). This strengthens our hypothesis following which the mass density profile of the OH GCS is tracing the cold baryonic material available to the star formation process some 15 Gyr ago.

An additional issue of potential concern is that a small, but non-negligible, fraction of the OH may itself be an accreted component. Several of the GCs in nearby dwarf galaxies have colour–magnitude diagram characteristics that are indistinguishable from OH GCs (see, e.g. Grebel & Gallagher 2004 and references therein). Furthermore, Mackey & Gilmore (2004) emphasize that, although the overwhelming contribution of clusters from external galaxies would be to the Galactic YH subsystem, there may also be a non-zero contribution to the OH subsystem, which they estimate of order 15 per cent or, equivalently, a dozen of GCs. Such accreted OH cluster candidates may be identified on the basis of either an extended core radius or spatial motions more typical of YH objects, although these alone are not definite indicators of an extra-Galactic origin. Mackey & Gilmore (2004) find five OH GCs in the first category (NGC 6809, 6101, 7492, 5897 and Pal 15) and six GCs in the second (NGC 1904, 2298, 5024, 5904, 6205, 7089). We have thus refitted equation (8) to the observed OH distribution, after rejecting (1) the five GCs with extended structure and (2) all 11 GCs quoted above plus Pal 2 (see below). These two observed spatial distributions are illustrated in Fig. 4. In the first case (filled symbols), one hardly detects a difference with respect to the distribution of the whole OH GCS (as in Figs 1–3). Accordingly, the parameters of the fit are much similar to previously [compare case (a) and case (b) in Table 3]. In a second step [open symbols in Fig. 4 and case (c) in Table 3], we have removed the complete sample of 11 OH GCs suspected of having been accreted as well as Pal 2. In the [Fe/H] versus HBR diagram, this one is located at the frontier between the OH and the YH groups and its nature is thus ill determined. While we have previously considered it to be an OH GC, we now sort it in the YH group. Removing the so-defined sample of 12 GCs, the changes are more significant but still, the modified observed distribution is satisfactorily fitted by equation (8), the main point being that the model distribution overestimates the mass density of the OH subsystem

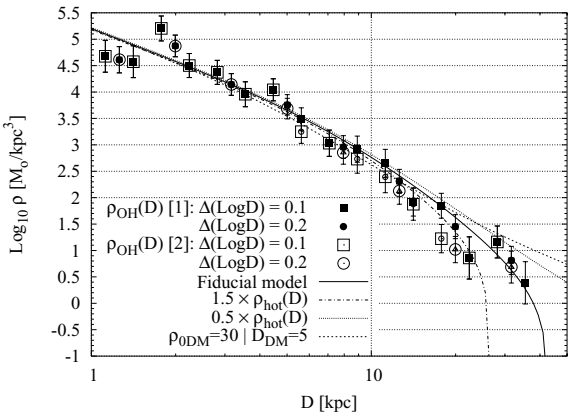

Figure 4. Comparison between the same set of curves as in the previous figure and the spatial distribution of the OH subsystem modified in the following way: exclusion from the initial sample of the GCs with extended structures (filled points) and of the GCs with kinematics more typical of the YH (open points).

in the region $D \simeq 20$ kpc. We thus conclude that our fit is robust, even though the actual radial distribution of the OH mass remains slightly uncertain as a few old clusters may be accreted objects and, thus, interlopers with respect to the genuine initial Galactic GCS.

In what follows, we consider the OH mass distribution displayed in Figs 1–3 and equation (8) as our fiducial observed and theoretical radial mass density profiles, respectively.

4 EVOLUTION OF THE SPATIAL DISTRIBUTION OF THE OH MASS

As announced in Section 2, we now put on a firmer foot the hypothesis following which the initial GCS mass density profile is reasonably approximated by what it presently is.

Evolutionary processes act more efficiently upon low-mass GCs as well as on GCs located in the inner Galactic regions. In other words, the evolution with time of the GCS has been mostly determined by the initial spatial distribution of the clusters in the Galactic halo as well as by their initial mass spectrum. In this respect, it is interesting to note that the sharp contrast between the fraction of surviving clusters and the ratio of the final to the initial total mass in clusters as obtained by McLaughlin (1999) (see Section 2) arises from the choice of a power-law mass spectrum with a steep (i.e. -2) slope and probing down to very low mass (i.e. of order $10^3\,M_\odot$). Other mass spectra could thus lead to different results.

How the initial mass spectrum of the Galactic halo GCs looked like is a much debated issue. As mentioned earlier, the observed luminosity spectrum dN/dL of numerous cluster systems recently formed in starburst and merging galaxies is a power law. However, whether the luminosity spectrum dN/dL constitutes a faithful mirror of the underlying mass spectrum dN/dm is questionable. Both shapes agree only if the variations of the mass-to-light ratio from cluster to cluster are limited (as is roughly the case for the Galactic halo GCS). Such a requirement may not be true for ongoing or recent starbursts: the formation duration of such systems may be a significant fraction of the median age of the system and, thus, age spread effects among the young star cluster population may not be negligible. Being an age-related quantity, the mass-to-light ratio can no longer be considered as a constant and the shape of the luminosity spectrum may differ substantially from the shape of the mass spectrum. Raising this issue, Meurer et al. (1995) and Fritze-von Alvensleben (1998, 1999) showed that systems of young GCs could display a power-law luminosity spectrum while the underlying mass spectrum is a broken power law or, equivalently, a Gaussian when the binning is logarithmic (dN/d log$m$). The reason for this is that, owing to the fading with time of the cluster luminosity, high-mass clusters can be observed over a wide range of ages, while low-mass ones are detectable at young ages only. As a result, low-mass clusters are underrepresented in the observed mass spectrum. Thus, this one can be described by a two-index power law (or equivalently a bell-shaped mass function) as it does not increase in the low-mass regime as steeply as in the high-mass regime.

Vesperini (1998) has indeed shown that the halo GCS could have started with a Gaussian initial mass function. Building on N-body simulations performed by Vesperini & Heggie (1997), he demonstrated the existence of a quasi-equilibrium GC mass function, that is, a mass function whose initial Gaussian shape and parameters (mean and standard deviation) are preserved during the entire evolution through a subtle balance between the disruption of clusters and evolution of the masses of those which survived, even though a significant fraction of the GCs is destroyed. Interestingly, the mean and the standard deviation of this Gaussian equilibrium mass function ($\log(m/M_\odot) = 5.03$ and $\sigma = 0.66$) are remarkably close to those of the mass function of the halo GCS. Thus, the initial GC mass function may have been very similar to what it is today. Obviously, the study of the temporal evolution of the GC mass spectrum is not enough to unveil its initial shape as both a power law and Gaussian mass functions evolve into the current GC mass function after a Hubble time.

If we *assume* that the halo GC initial mass spectrum was similar to what is observed today in starbursts and mergers, to derive the latter, one should estimate the individual ages for all star clusters. This can be done by, for instance, comparing the observed broad-band photometry to the colours generated by spectral evolution synthesis models (see, e.g. Parmentier, de Grijs & Gilmore 2003). These models will then provide an estimate of the mass-to-light ratio for each cluster as a function of age, eventually enabling one to derive the intrinsic mass spectrum underlying the observed luminosity spectrum. Unfortunately, even such studies lead to inconclusive results. Analysing the system of young GCs in the Antenna merger NGC 4038/39, Zhang & Fall (1999) show that the very young clusters (i.e. with age less than 150 Myr), those which have remained unaffected by the various dynamical effects, are distributed in mass according to a pure power law with slope -2. On the other hand, de Grijs et al. (2003) derive a Gaussian mass function dN/dlog$m$ (or equivalently a two-index power law when binning the data in m) for an equally young system in the nearby starburst galaxy NGC 3310.

Therefore, at the present stage, neither the theory of the dynamical evolution of a GCS, nor the observations of young GCs in starburst galaxies can help distinguishing between a power law or a Gaussian mass function for the GC initial population. Considering the very unclear issue of this debate, we have computed the temporal evolution of the spatial distribution of the GCS mass around the Galactic centre for various mass functions.

To evolve the spatial distribution of the mass of a GCS from the time of its formation up to an age of 15 Gyr, we adopt the analytic formulae of Vesperini & Heggie (1997) which supply at any time t the mass m of a GC with initial mass m_i and moving along a circular orbit at a galactocentric distance D. These relations have been obtained by fitting the results of a large set of N-body simulations in which Vesperini & Heggie (1997) take into account the effects of stellar evolution as well as two-body relaxation, which leads to evaporation through the GC tidal boundary. Disc shocking can also

be included (see below). In order to take into account dynamical friction, GCs whose time-scale of orbital decay (see, e.g. Binney & Tremaine 1987) is smaller than t are removed from the GCS at that time. A summary of the method is provided in Vesperini (1998, his Section 2).

The temporal evolution of the mass of a GC, modelled as a multimass King model with an initial dimensionless concentration parameter $W_0 = 7$ and orbiting at constant galactocentric distance D, is assumed to follow:

$$\frac{m(t)}{m_i} = 1 - \frac{\Delta m_{\rm st,ev}}{m_i} - \frac{0.828}{F_{\rm cw}} t. \quad (9)$$

$\Delta m_{\rm st,ev}/m_i$ is the fraction of cluster mass lost owing to stellar evolution (18 per cent in this particular model). The time t is expressed in units of 1 Myr and $F_{\rm cw}$, a quantity proportional to the initial relaxation time, is defined as

$$F_{\rm cw} = \frac{m_i D}{\ln N}, \quad (10)$$

where m_i and D are in units of 1 $M_\odot$ and 1 kpc, respectively, and N is the initial number of stars in the GC. To take into account disc shocking, the factor $0.828/F_{\rm cw}$ is merely replaced by λ as defined by equation (3) of Vesperini (1998).

We have distributed 20 000 GCs following a radial distribution obeying our equation (8) and various mass spectra

(i) a Gaussian mass function dN/dlog$m$ with parameters equal to those of the equilibrium mass function of Vesperini (1998),

(ii) three power-law mass spectra dN/dm with a single slope of –1.9 and different lower mass limits, namely, 1E3, 1E4 and 1E5 $M_\odot$.

As for the last cut-off value, Fall & Zhang (2001) indeed showed that the GC mass spectrum might have started with a truncation at mass of order 1E5 $M_\odot$, the low-mass tail of the currently observed GC mass distribution being formed as a result of the evaporation of the massive GCs located at short distance from the Galactic centre.

Each panel of Fig. 5 displays the results of one of these simulations (the case of a power law truncated at 1E4 $M_\odot$ is not represented as it is highly similar to the 1E3 $M_\odot$ case). The dashed, plain and dashed-dotted lines are, respectively, the initial mass density profile as described by equation (8), the radial mass density profile after a Hubble time long evolution without disc shocking (obtained through equation 9) and with disc shocking. The final profile without disc shocking (plain curve) has been vertically shifted to provide the best agreement, in the least-squares sense, with the observed spatial distribution of the OH mass. The amplitude $\Delta\log_{10}\rho$ of the shift, the χ^2 and Q values of each fit, as well as the fraction of surviving clusters (F_N) and the ratio of the final to the initial total mass in GCs (F_M), are listed in Table 4. F_N exhibits an extremely large range of variation, with more than 90 per cent of the clusters being disrupted if the initial mass spectrum is a single power law going down to 1000 $M_\odot$, while a cut-off at 10^5 $M_\odot$ leads to the preservation of most of the GCs. This large scatter in F_N contrasts markedly with the limited range in F_M, as this one varies by less than a factor of 2. Therefore, considering our ignorance of the shape of the GC initial distribution in mass, mass-related quantities appear as indicators of the initial conditions more reliable than number-related quantities. In the framework of the initial density profile described by equation (8), we also note that the initial mass of the OH GCS was at most 2.5 times larger than what it currently is, thus suggesting that the bound cluster formation efficiency in the Galactic halo was at most of order $2.5 \times (2 \times 10^{-4})$. This result also agrees with previous studies (e.g. Baumgardt 1998; Vesperini 1998; McLaughlin 1999)

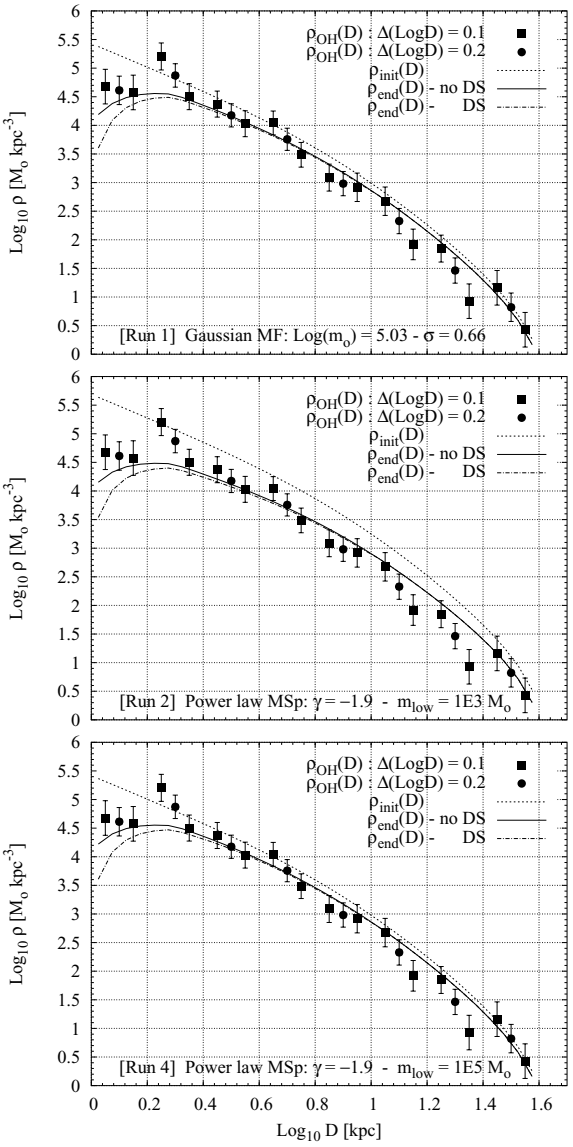

Figure 5. Evolution with time of the radial mass density profile of a GCS whose mass is initially spatially distributed according to equation (8) (dashed curve). Results with (dashed-dotted curve) and without (plain curve) disc shocking are shown for three different initial GC mass spectra. The plain curve is vertically shifted to match the observed data (see the quantity $\Delta\log_{10}\rho$ in Table 4).

following which the disruption of GCs cannot be a major contributor to the build-up of the stellar halo. Indeed, assuming a mass-to-light ratio of 2.35 (see Section 2), the mass of the OH GC subsystem is $\simeq 2 \times 10^7$ $M_\odot$, about two orders of magnitude less massive than the stellar halo ($\simeq 10^9$ $M_\odot$, Freeman & Bland-Hawthorn 2002).

As already quoted, the shapes of the initial and final mass profiles are very similar, at least beyond a galactocentric distance of $\simeq$2 kpc. It may be worth remembering that about one fifth of the cluster mass decrease is owing to mass-loss associated with stellar evolution, which is independent of galactocentric distance. As a result, the shape of the radial profile is left unaffected by this gaseous mass loss taking place during the very early evolution of the GCs. The initial shape of the model profile being only moderately affected by dynamical evolution, it is not surprising that the observed OH profile (indicated by the filled squares or circles in Fig. 5, depending on the

Table 4. Results of our simulations for different GC initial mass functions (see text for details). F_N and F_M are the fraction of surviving GCs and the ratio of the final to the initial mass in GCs, respectively. Also given are the results of fitting the radial distributions evolved during 15 Gyr to the data for the two different binnings considered, that is, the vertical logarithmic shift $\Delta\log_{10}\rho$ required to obtain the best match between the model and the data and the corresponding χ^2 and Q($\nu/2$, $\chi^2/2$) values.

Run	GC IMF	F_N	F_M	$\Delta\log_{10}D = 0.1$			$\Delta\log_{10}D = 0.2$		
				$\Delta\log_{10}\rho$	χ^2	Q	$\Delta\log_{10}\rho$	χ^2	Q
[1]	Gaussian (Mean = 5.03; $\sigma = 0.66$)	0.75	0.66	−2.11	20.7	0.15	−2.14	7.1	0.40
[2]	Power law ($m_{\rm low} = 10^3\,{\rm M}_\odot$)	0.06	0.39	−0.54	27.3	0.03	−0.56	10.9	0.14
[3]	Power law ($m_{\rm low} = 10^4\,{\rm M}_\odot$)	0.46	0.51	−1.44	27.2	0.03	−1.46	10.9	0.14
[4]	Power law ($m_{\rm low} = 10^5\,{\rm M}_\odot$)	0.96	0.68	−2.30	20.4	0.16	−2.31	6.9	0.44

size of the bins) and the outcome of our simulations (plain curve in Fig. 5) are in satisfactory agreement as indicated by the Q values listed in Table 4. The agreement is weaker than in Table 3 however, especially for the power laws with a truncation at 1E3 $\rm M_\odot$ and 1E4 $\rm M_\odot$, but this effect is mostly driven by one bin only, at $\log D = 0.25$. Should it be ignored, the agreement between the model and the observations would jump up to $Q \simeq 0.3$ in the least favourable cases. This kick in the observed density profile arises from the presence, at almost the same galactocentric distance, of two of the handful of very massive ($M_{\rm v} \simeq -9.2$) GCs, i.e. NGC 6266 and 6273 at $D =$ 1.7 and 1.6 kpc, respectively.

In the case of disc shocking (dashed-dotted curves in Fig. 5), the ratios F_N and F_M are almost unaffected, being reduced by 4 per cent at most with respect to the simulations without disc shocking (see Table 4). The shape of the density profile is also preserved except at galactocentric distances shorter than 2 kpc where the predicted cluster density is significantly affected compared to the case without disc shocking. In these regions, the disc shocking model underestimates the observed mass density. This discrepancy may be solved if these very inner halo regions are contaminated by the metal-poor tail of the bulge GCS. Alternatively, it may be that the high-density high-pressure environment of these very inner Galactic regions promoted the formation of GCs with an efficiency locally higher than in the overall halo. In such case, the original GCS mass density profile around the Galactic centre may have been steeper than the density profile $\rho_{\rm cold}$.

It is interesting to compare the values F_N and F_M listed in Table 4 with those obtained in previous studies. Considering the case of the equilibrium GC mass function (run [1] in Table 4), Vesperini (1998) derived $F_N \simeq 0.55$ and $F_M \simeq 0.40$. As for a power-law mass spectrum with a slope −2 and a low-mass cut-off $\sim$1000 $\rm M_\odot$ (run [2] in Table 4), Baumgardt (1998) indicates that the fraction of surviving clusters may be of order 1 per cent, while the final mass in GCs would represent 15–30 per cent of the initial mass content. These results, although in rough agreement with ours, are systematically lower. This is not surprising, however, as these studies assume an initial radial distribution scaling as $D^{-3.5}$ (even $D^{-4.5}$ for some of Baumgardt's runs), thus significantly steeper in the inner regions than our radial profile $\rho_{\rm cold}$ (see Fig. 2). Therefore, with respect to our simulations, a larger fraction of the initial population of GCs is put on orbits closer to the Galactocentric centre where they are more efficiently evaporated and eventually disrupted.

5 DISCUSSION AND SUMMARY

We have proposed a model accounting for the spatial distribution of the mass of the OH GCS. We suggest that this GC subsystem formed out of the cold baryonic gas present in the Galaxy some 15-Gyr ago, that is the gas leftover once the contribution of the dark matter is removed, with a roughly constant formation efficiency throughout the halo. In order to test our hypothesis, we have built the presently observed radial distribution of the OH GCS, making use of the latest classification of the halo GCs between the OH and YH subsystems (Harris 1996, updated 2003, Mackey & Gilmore 2004). We have found good agreement between our suggested model (equation 8) and the observed OH mass distribution (see Fig. 2 and Table 3). The fit is robust with respect to uncertainties in the observed distribution of the mass (i.e. depending on whether a few OH GCs may be accreted objects as the YH GCs) as well as with respect to the uncertainties in the parameters involved in equation (8).

We have made one more step, demonstrating that the GCS mass density profile, as described by equation (8), has not been severely affected by a Hubble time long evolution in the tidal fields of the Milky Way, at least beyond galactocentric distances of order 2–3 kpc. This result is only weakly dependent on the shape of the initial GC mass spectrum, which is still very poorly known. In fact, numerous studies found that both an initial Gaussian mass function (i.e. a two-index power-law mass spectrum) and an initial power-law mass spectrum will evolve into the presently observed Gaussian mass function of GCs. Therefore, to recover the faint end of the original mass function of GCs on the basis of its temporal evolution only is not feasible. We have thus considered various mass functions in order to demonstrate the robustness of the GCS mass density profile with respect to dynamical evolution.

Our simulations make use of the analytic formulae obtained by Vesperini & Heggie (1997), and the starting point consists in assuming a given radial distribution and a given mass function for the GCs. In doing so, we neglect finer details such as the non-circularity of the GC orbits as well as the initial concentration of GCs. As for the first point, however, we recall that our main interest in this paper is the OH subsystem, which shows less extreme kinematics than the YH GCs (see e.g. Dinescu et al. 1999). Thus, while the assumption of circular orbits for the GCs is clearly a simplifying one, this issue is likely to be less critical than if we have dealt with the whole halo GCS or with the YH only. Regarding the second point, we note that equation (9), which describes the temporal decrease of the cluster mass according to Vesperini & Heggie (1997), implicitly assumes an initial concentration $W_0 = 7$ for all GCs. The existence of GCs with lower initial concentration is thus clearly neglected. Such low-concentration GCs may have been initially present and destroyed relatively quickly by a combination of stellar winds and tidal limitation with little or no help from two-body relaxation or gravitational shocks. In the inner Galactic regions (say within the Solar Circle), that is, where most of the GCS mass is located, even high-mass GCs are unable to survive if their initial concentration is low (Vesperini & Heggie 1997). By assuming that all GCs start with a concentration $W_0 = 7$, we may thus overestimate the survival capacity of some high-mass GCs and, thus, underestimate the decrease with time of $\rho_{\rm OH}(D)$. However, it is worth pointing out that GCs exhibit a correlation between their luminous mass estimate and their concentration

in the sense that more massive GCs are more concentrated (van den Bergh 1994). This correlation is likely to be of primordial origin as it is stronger at larger galactocentric distances (Bellazzini et al. 1996), that is, where evolutionary processes act on longer time-scales and, thus, where memory of the initial conditions is better preserved. Moreover, simulations show that high-mass low-concentration GCs are destroyed in the inner halo but manage to survive at large galactocentric distances (i.e. $D \gtrsim 10$ kpc, Vesperini & Heggie 1997). As they are not observed even beyond the Solar Circle, high-mass low-concentration GCs were probably not part of the initial GCS and, therefore, to neglect them should not affect the results displayed in Fig. 5 and Table 4.

Bearing these caveats in mind, we have shown that the shape of the evolved radial mass density profile still nicely mirrors the initial one, even though a significant fraction of the GCs has been destroyed during a Hubble time long evolution. Not surprisingly thus, the observed spatial distribution of the OH mass and the distributions arising out of our simulations are also found to be in good agreement (see Fig. 5 and Table 4). This strengthens our hypothesis following which the distribution of the gas GCs formed obeys equation (8) and, also, that the dark matter, whatever its nature, was not involved in the earliest stages of star formation.

This good agreement also suggests that the flattening of the observed distribution of GCs around the Galactic centre may not result from tidal disruption processes only but may be, at least partly, of primordial origin. Indeed, in the region 1–3 kpc, our suggested cold matter profile shows a flattening (slope $\simeq -2$) which contrasts with the overall shape, reasonably approximated by a slope of $\simeq -3.5$ (see Fig. 2). The situation is still unclear, however as, at an age of 15 Gyr, our mass distribution underestimates the observed mass density profile of the GCS for $D \leqslant 2$ kpc, especially when disc shocking is included in the simulations (see Fig. 5). Possible solutions of this discrepancy include the contamination of the observed distribution by the metal-poor tail of the bulge/disc system and/or star formation efficiencies higher in the inner regions of the Galaxy owing to higher pressures and densities. As a result of this latter suggestion, the initial mass distribution of the GCs in the Galactic central regions may have been steeper than indicated by equation (8). Apart from these uncertainties, the satisfactory agreement between the model and the observed radial density profile of the OH subsystem, beyond $D \simeq 2$–3 kpc, suggests that the formation of GCs took place with a formation efficiency almost constant throughout the OH.

REFERENCES

Baumgardt H., 1998, A&A, 330, 480
Bellazzini M., Vesperini E., Ferraro F. R., Pecci F., 1996, MNRAS, 279, 337
Binney J., Tremaine S., 1987, Galactic Dynamics. Princeton Univ. Press Princeton NJ
Caldwell J. A. R., Ostriker J. P., 1981, ApJ, 251, 61
Da Costa G. S., Armandroff T. E., 1995, AJ, 109, 2533
de Grijs R., Fritze-v. Alvensleben U., Anders P., Gallagher J. S., Bastian N., Taylor V. A., Windhorst R. A., 2003, MNRAS, 342, 259
Dehnen W., Odenkirchen M., Grebel E. K., Rix H.-W., 2004, AJ, 127, 2753
Dinescu D. I., Girard T. M., Van Altena W. F., 1999, AJ 117, 1792
Djorgovski S., Meylan G., 1994, AJ, 108, 1292
Eggen O. J., Lynden-Bell D., Sandage A., 1962, ApJ, 136, 748
Fall S. M., Rees M. J., 1985, ApJ, 298, 18
Fall S. M., Zhang Q., 2001, ApJ, 561, 751
Freeman K. C., Bland-Hawthorn J., 2002, ARA&A, 40, 487
Fritze-von Alvensleben U., 1998, A&A, 336, 83
Fritze-von Alvensleben U., 1999, A&A, 342, L25
Gnedin O. Y., Ostriker J. P., 1997, ApJ, 474, 223
Grebel E. K., Gallagher J. S., III, 2004, ApJ, 610, L89
Harris W. E., 1996, AJ, 112, 1487
Harris W. E., Pudritz R. E., 1994, ApJ, 429, 177
Harris W. E. et al., 1997, AJ, 114, 1030
Lee Y. W., Demarque P., Zinn R., 1994, ApJ, 423, 248
Mackey A. D., Gilmore G., 2004, MNRAS, 355, 504
McLaughlin D. E., 1994, PASP, 106, 47
McLaughlin D. E., 1999, AJ, 117, 2398
McLaughlin D. E., Pudritz R. E., 1996, ApJ, 457, 578
Meurer G. R., Heckman T. M., Leitherer C., Kinney A., Robert C., Garnett D. R., 1995, AJ, 110, 2665
Murray S. D., Lin D. N. C., 1992, ApJ, 400, 265
Odenkirchen M. et al., 2001, ApJ, 548, L1650
Parmentier G., Gilmore G., 2001, A&A, 378, 97
Parmentier G., Jehin E., Magain P., Noels A., Thoul A., 2000, A&A, 363, 526
Parmentier G., de Grijs R., Gilmore G., 2003, MNRAS, 342, 208
Piotto G. et al., 2002, A&A, 391, 945
Press W. H., Teukolsky S. A., Vetterling W. T., Flannery B. P., 1992, Numerical Recipes, 2nd edn. Cambridge Univ. Press, Cambridge
Pryor C., Meylan G., 1993, in Djorgovski S. G., Meylan G., eds, ASP Conf. Ser. Vol. 50, Structure and Dynamics of Globular Clusters. Astron. Soc. Pac., San Francisco, p. 370
Salaris M., Weiss A., 2002, A&A, 388, 492
Searle L., Zinn R., 1978, ApJ, 225, 357
van den Bergh S., 1993, ApJ, 411, 178
van den Bergh S., 1994, ApJ, 435, 203
van den Bergh S., 2000, The Galaxies of the Local Group. Cambridge Univ. Press, Cambridge
van den Bergh S., Mackey A. D., 2004, MNRAS, 354, 713
Vesperini E., 1998, MNRAS, 289, 898
Vesperini E., Heggie D. C., 1997, MNRAS, 289, 898
Whitmore B. C., Schweizer F., 1995, AJ, 109, 960
Whitmore B. C., Schweizer F., Kundu A., Miller B. W., 2002, AJ, 124, 147
Zhang Q., Fall S. M., 1999, ApJ, 527, L81
Zinn R., 1985, ApJ 293, 424
Zinn R., 1993, in Smith G. H., Brodie J. P., eds, ASP Conf. Ser. Vol. 48. The Globular Clusters–Galaxy Connection. Astron. Soc. Pac., San Francisco, p. 38

This paper has been typeset from a TEX/LATEX file prepared by the author.